

Piezoelectric active sensing system for crack detection in concrete structure

Chen Zhang¹ · Xun Yu^{1,2} · Lee Alexander³ · Ye Zhang³ · Rajesh Rajamani³ · Navneet Garg⁴

Received: 14 March 2015 / Revised: 17 September 2015 / Accepted: 19 September 2015 / Published online: 29 February 2016
© Springer (outside the USA) 2016

Abstract This paper presents an active piezoelectric sensing system for concrete crack detection that is based on the energy diffusivity method. The feasibility of using the energy diffusivity of ultrasound to characterize the structural integrity of a pavement is first analyzed. Experiments are then carried out to evaluate the performance of this approach to crack detection. In addition, the detectable range of this system is studied by testing it with cuttings at different angles and different distances between sensor and actuator. Results show that by analyzing the energy diffusivity density of the sensor responses, cracks in the concrete specimen can be detected. This crack detection system can be used in highway and airport pavement slabs for pavement health monitoring applications.

Keywords Piezoelectric · Active sensing system · Energy diffusivity · Detectable range · Pavement health monitoring

1 Introduction

As one of the most important areas in health monitoring of concrete structures, crack detection techniques have been studied for many years [1–4]. Various crack detection techniques have been proposed, including manual visual survey, image analysis-based approaches and ultrasonic measurement-based approaches [3–11]. Traditional manual visual checks are associated with disadvantages of high labor cost, low accuracy and low reliability, especially for cracks that do not appear on the surface of pavements [12]. Image-based analysis is mainly employed to detect the cracks that have already appeared on the surface of pavements. In recent years, the piezoelectric-based sensing system [13–17] has attracted a lot of research interest as it offers a relatively inexpensive and reliable method to monitor the health status of concrete structures, including internal crack growth. A piezoelectric-based sensing system is also known as a nondestructive tool due to its relatively small size and thus flexibility to be integrated into the concrete structures. In addition, a piezoelectric sensing system is more accurate and its response can be quantitatively described due to its mechanical–electrical coupling property, due to which physical structure changes induce electrical signals [15–18].

Based on different types of ultrasonic wave propagation, piezoelectric active sensing systems for concrete pavements can be divided into two major categories: impedance-based methods and lamb wave-based methods. The impedance-based method employs acoustic impedance as the index to evaluate health status and detect cracks [11, 14, 16]. Similar to common acoustic waves, ultrasonic waves will be reflected, deflected and scattered due to the inhomogeneity of the medium, especially at the boundary between different mediums. The inhomogeneity of the

✉ Xun Yu
xyu13@nyit.edu

¹ Department of Mechanical and Energy Engineering, University of North Texas, Denton, TX 76203, USA

² Department of Mechanical Engineering, New York Institute of Technology, Old Westbury, NY 11568, USA

³ Department of Mechanical Engineering, University of Minnesota, Minneapolis, MN 55455, USA

⁴ William J. Hughes Technical Center, Federal Aviation Administration, Atlantic City, NJ 08405, USA

mediums will result in the inconformity of the impedance by which crack detection could be implemented. Considering that a typical concrete pavement is a plate-like structure where one dimension (depth, usually in several inches) is significantly smaller than the other two dimensions (length and width), the Lamb wave-based method can also be applied for crack detection. According to symmetry, Lamb waves can be specified in two modes, symmetric mode (S0) and antisymmetric mode (A0). The symmetric mode is also called a longitudinal wave while the antisymmetric mode is referred to as a flexural mode. The Lamb wave method is focused on ultrasonic wave propagation itself where piezoelectric transducers [e.g., lead zirconium titanate (PZT)] are employed as both the actuator and sensor. The actuator is excited and generates an ultrasonic wave that transmits in the concrete and is received by the sensor which will then produce a response signal. Therefore, a crack could be detected by comparing the sensor response to the baseline which is tested during healthy status of the pavement [9, 12, 13]. To use this method, the propagation distance, from actuator to sensor, has to be determined to be within a specific range for mode separation as well as for minimizing interference effects from reflections.

Previous studies of piezoelectric-based sensing systems have indicated that both impedance-based and Lamb wave-based approaches are used in energy diffusion. The impedance-based approach is engaged in the energy transfer between actuator and concrete specimen while the Lamb wave-based approach is used to reveal the energy transformation between actuator and sensor. However, these two approaches are mainly focused on the signal transmission between actuators and sensors but ignore the energy diffusivity property of ultrasound. This might be due to the complexity of the wave propagation in concrete structures and lack of effective mathematical models to evaluate the ultrasound energy density in concrete.

The propagation of a mechanical wave in a heterogeneous elastic body is associated with attenuation [19–21]. There are two major mechanisms of attenuation in such bodies: diffusion (incoherent) due to viscosity, relaxation, elastic hysteresis, etc.; and dissipation (coherent) due to inhomogeneity. Additional ultrasonic wave attenuation is caused by absorptive mechanism in which mechanical vibration is absorbed in the material mostly due to its viscoelastic characteristics. It has been shown that the traditional coherent ultrasonic attenuation measurement cannot distinguish between these two mechanisms [20, 21]. Therefore, a new approach that can separate dissipation (coherent) and diffusion (incoherent) energy is required. Compared with other materials, such as steel and iron, concrete is more heterogeneous since it is a mixture of cement, sand and water which will lead to heavier

ultrasonic wave attenuation. Considering this, an energy-based testing method is proposed to analyze the diffusion of ultrasonic waves and use it to monitor the structural health of concrete pavement. Experiments were carried out to evaluate this proposed approach.

2 Energy diffusivity of ultrasound propagation

Energy diffusivity of ultrasound has come into the sight of researchers for several years. Several research papers reported the efforts of studying ultrasound diffusion and its application. Frederik et al. [19] applied diffuse ultrasound to detect damage in concrete in 2010, and Phanidhar et al. [18] have studied diffusion of ultrasound in concrete in 2001. Ramamoorthy et al. [22] conducted crack depth determination in concrete using ultrasound diffusion in 2004. Besides the application to concrete structures, ultrasound diffusion can also be applied to the nondestructive characterization of other materials. Weaver [23, 24] has discussed the propagation of ultrasonics in aluminum foam which is focused on the nondestructive characterization of materials with strongly scattering microstructures. However, previous studies in ultrasound diffusivity mentioned above are mainly based on the propagation velocity or focused on the time domain and few of them paid attention to its energy transmission during propagation.

For a given concrete structure, the energy losses for ultrasonic wave propagation will be mainly affected by its diffusivity, which is a quantitative reflection of the homogeneity state of the concrete. Considering this, there is a great possibility to employ ultrasonic diffusivity, in terms of energy loss, as the index of concrete structure health monitoring. Experiments were carried out to examine the relationship between energy losses and cutting size (depth in this paper). To quantitatively describe the energy density for different cutting depths, energy diffusivity analysis was first proposed to evaluate the feasibility of such an application, then a Root Mean Square value of sensor's response was employed to indicate the energy status of ultrasound signal detected at the sensor.

3 Experiments

3.1 Experiment setup

To verify the performance of the diffusivity-based crack detection method, experiments were conducted and the experimental setup is shown in Fig. 1. The experimental setup includes a signal generator, signal amplifier, data acquisition device and transducers (piezoelectric-based

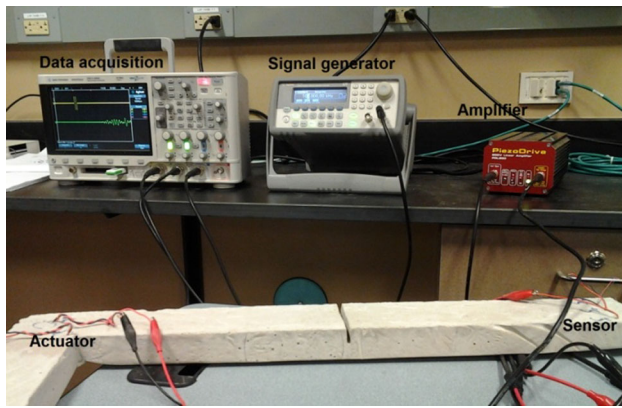


Fig. 1 Picture of the lab test setup

actuator/sensor). Figure 2 shows the physical size and position of the experimental components. The properties of the concrete specimen are shown in Table 1. It should be noted here that the specimen is made of concrete without any reinforcement. The extension of this sensing system to real concrete structures needs to be readdressed in the future. The actuators and sensor are commercial products and the properties of them are shown in Table 2. Both actuators and sensors are embedded into the concrete mixture before curing of the concrete. The excitation signal, consisting of 2 cycles of a sinusoidal signal, is generated by a signal generator (Agilent 33220A, 200 MHz function/arbitrary waveform generator) and amplified by a piezo drive amplifier (PD200), which is used to amplify the excitation signal to a detectable level. A longitudinal ultrasonic wave will then be excited to transmit through the concrete structure and will be received by the sensor by which mechanical vibrations will finally be transferred to an electrical signal. Both the excited and detected signals are recorded by the data acquisition equipment (Agilent MSOX3104T oscilloscope 1 GHz) and will be processed using digital signal processing (DSP) techniques.

A schematic diagram is shown in Fig. 3. To simulate natural crack damage, a crack is artificially created using a concrete saw cutting in the concrete and its depth is incrementally increased from 0" to 1" with an increment of 1/3" and a width of 0.15". For each cut depth, two different

excitation frequencies (50, 100 kHz) are applied to test the response signals.

3.2 Parameters determination

The determination of some important testing parameters is introduced and explained, including excitation frequencies and effective window width of sensor response.

3.2.1 Excitation frequencies

The excitation frequency has a large impact on the measurable distance range and crack size detection resolution. The transmission of ultrasonic signal inside the concrete is very complex. When an ultrasonic signal meets an obstacle, a crack, or a boundary, part of the signal will be reflected, part of the signal will scatter around the obstacle or the crack, and part of the signal will diffuse through the obstacle. The wavelength of the ultrasonic signal would have large influence on how much of the signal can scatter around the obstacle or the crack. Typically, if the 1/4th of wavelength is larger than the size of the obstacle or the crack, the signal would be able to scatter around the obstacle or the crack. In this research, to detect the crack inside the concrete, we would need the 1/4th wavelength of the signal to be less than the desired detectable crack size. Therefore, the higher the ultrasonic frequency, the smaller the wavelength, and then the smaller the detectable crack size. In concrete, the ultrasonic wavelength $\lambda = c/f$, where C is ultrasonic speed (around 3500 m/s in concrete) [25–27], f is the frequency of the ultrasonic signal. For instance, a 10 kHz signal would have a λ of 0.35 m (the detection resolution would be around $\lambda/4 = 8.75$ cm or 3.44"), a 50 kHz signal would have λ of 0.07 m (the detection resolution would be around $\lambda/4 = 1.75$ cm or 0.68"), and a 100 kHz signal would have λ of 0.035 m (the detection resolution would be around $\lambda/4 = 0.875$ cm or 0.34"). However, it should be noted that a high frequency ultrasonic signal would have shorter traveling distance, and thus would give short detectable range. Therefore, there is a trade-off between crack detection resolution and detectable distance from the actuator.

Fig. 2 Physical size and position of the experiment components

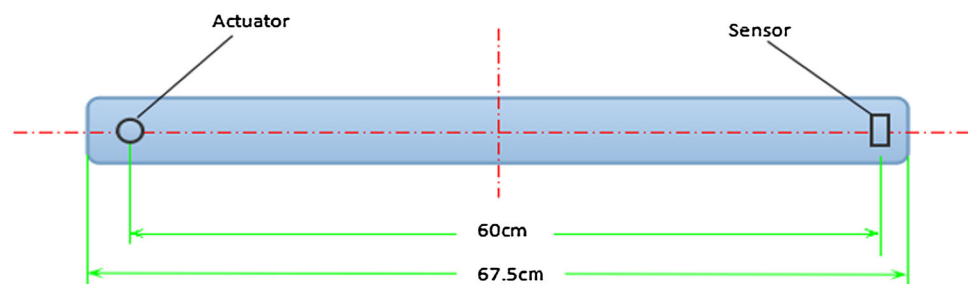
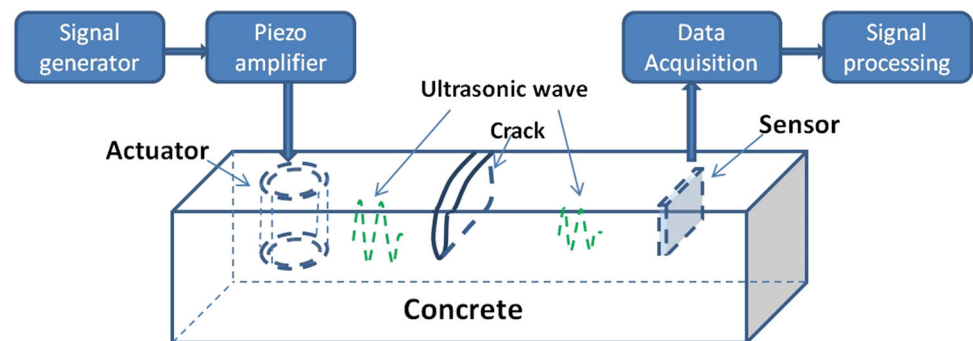


Table 1 Properties of concrete specimen

Made	W/C	Length	Width	Depth	Notch/depth	Age
Portland cement	0.38	67.5 cm	7.62 cm	2"	Max:0.5	>28 days

Table 2 Parameters of the used piezoelectric actuator and sensor

Type	Dimension	Resonant freq.	Piezo material
Actuator			
Piezoelectric ceramic cylinder	26 × 22 × 13 mm	43 kHz ± 1.5 kHz	SM111
Sensor			
Piezoelectric ceramic disc	25 × 0.7 mm	3 MHz ± 100 kHz	SM111

Fig. 3 Schematic diagram of the experiment procedure

In this research, 50 and 100 kHz signals are used. Moreover, instead of using continuous sinusoidal waves, short sinusoidal impulsive waves with 2 cycles were used in the tests, which give much better indication of the ultrasonic wave transmission process. The signal amplitudes are 0.5 v and the amplifier ratio is 20. The signals are sampled at the sampling rate of 100 MHz.

3.2.2 Effective window width of sensor response

Sensor outputs are much more complex than the excitation signals. This is due to the complex ultrasonic wave phenomena in the concrete. When the actuator sends out the excitation signal, a fraction of the ultrasonic wave will directly be transmitted through the concrete and reach the sensor which is the fastest route to the sensor, thus these are the first two waves of the sensor signal. Some other ultrasonic waves will be reflected and scattered back and forth by the boundaries and obstacles, thus will reach the sensor later. As the ultrasonic wave could bounce back and forth a couple of times before it totally dies out, even with a short impulse of excitation, the sensor will measure a long period of “tail” signal in addition to the firstly received ultrasonic signals. When there is a crack (cutting in the test), the ultrasonic signal will be attenuated by the cutting, thus the sensor will give different outputs, especially the first several waves on the sensor output. Therefore, to access the influence of cutting on the signal output, only the first few waves of the

sensor signals are analyzed. A window width of one of the two-cycle excitation signal period is too short to cover all the effective sensor response while three or more times of the period will include much more noise. So for quantitative calculations, the window is set to be twice of the two-cycle excitation signal period, which covers the major effective part of the sensor response and minimizes the noise generated from scattering and reflection.

4 Results and discussion

4.1 Signal analysis

The sensor responses to different cutting depths for different excitation frequencies (50, 100 kHz) were measured. Figure 4 shows the excitation signal and sensor responses of different cutting depths with an excitation signal of 50 kHz sent to the actuator. The top subplot of Fig. 4 shows the excitation signal, and the bottom subplot of Fig. 4 shows the sensor outputs with different cutting depths in the concrete beam. Figure 5 shows a similar test, except the excitation signal is 100 kHz. From Figs. 4 and 5, compared to the impulse excitation signals, the sensor signals have long “tails” as explained above. The sensor responses reduced significantly with the increase of cutting depth for both excitation frequencies, while 100 kHz gives larger magnitude changes with cuttings which means

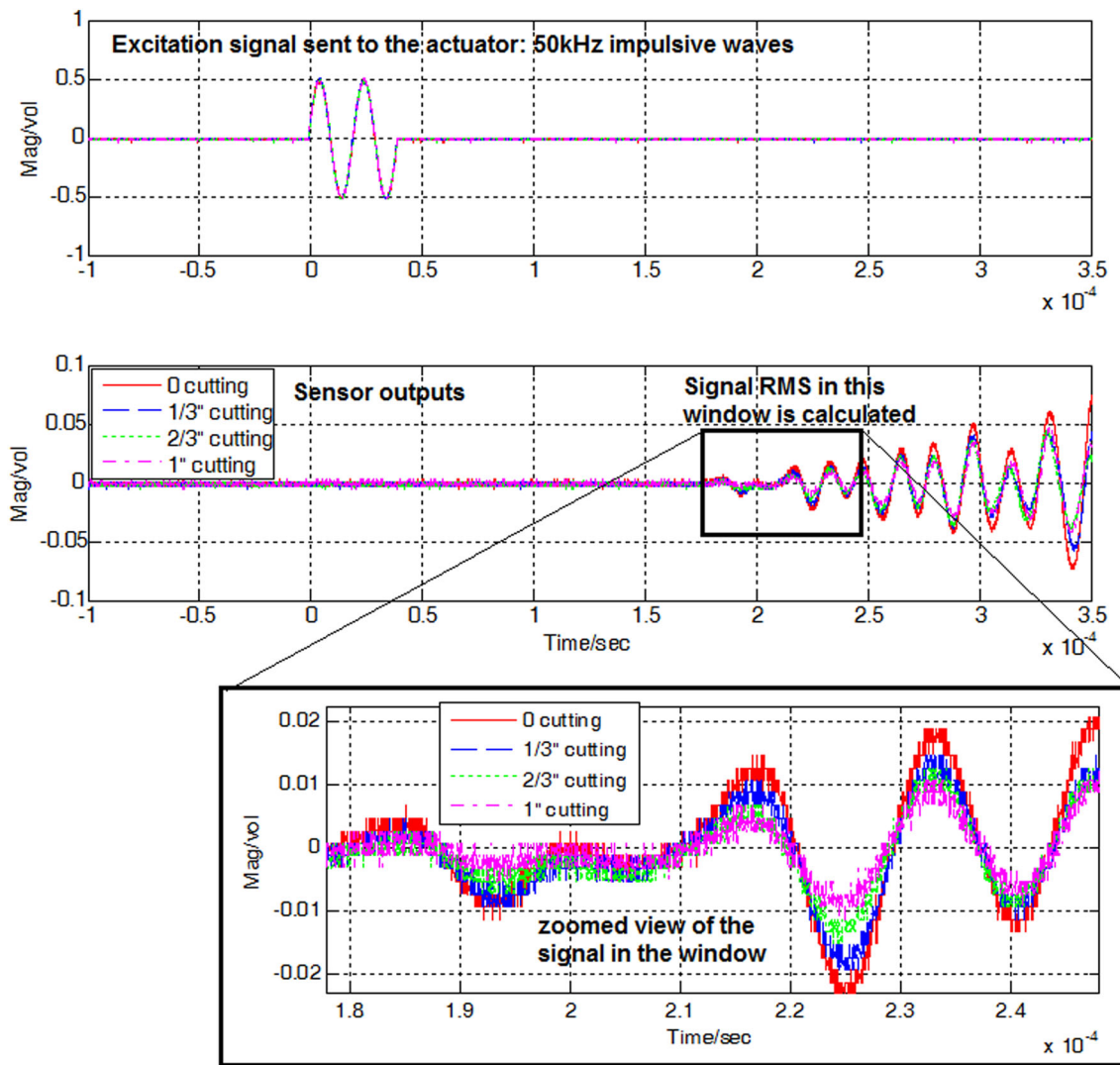


Fig. 4 Excitation signal and sensor response for 50 kHz excitation frequency

higher frequency signal gives higher resolution. However, comparing Fig. 4 with Fig. 5, the sensor responses to 100 kHz excitation give smaller magnitude comparing to the one from 50 kHz excitation, which is due to larger wave attenuation of the higher frequency wave that has smaller wavelength. Thus, a higher frequency will have a smaller detectable distance range.

4.2 Energy diffusivity analysis

Because an ultrasonic wave will be attenuated by heterogeneity of the concrete structure, a method based on energy diffusion will be more effective at crack detection, compared to the analyzing of specific properties of Lamb waves. Typically, the energy diffusion of ultrasonic waves propagating in a healthy concrete can be modeled by a one-dimensional diffusion equation with dissipation which does

not consider the geometry or dimensions of the concrete structure. The equation is given by [18, 21–24, 28]:

$$\frac{\partial E(x, y, t)}{\partial t} = D \nabla^2 E(x, y, t) - \sigma E(x, y, t) + P(x, y, t) \quad (1)$$

where $E(x, y, t)$ is ultrasonic spectral energy density (energy per volume, per frequency bandwidth); D is frequency-dependent ultrasonic diffusivity (with dimension of length squared per time); σ is absorptivity of concrete (with dimension of inverse time); and P is the excitation spectral power density (i.e. the input pulse). P is concentrated in space and time for a point impulsive source and can be modeled as Dirac delta function δ . When considering the geometry and dimensions of the concrete structure, a two-dimensional diffusivity equation with dissipation can be determined to model the diffusion of ultrasonic energy in a healthy concrete structure. The two-dimensional equation is then given by [18]:

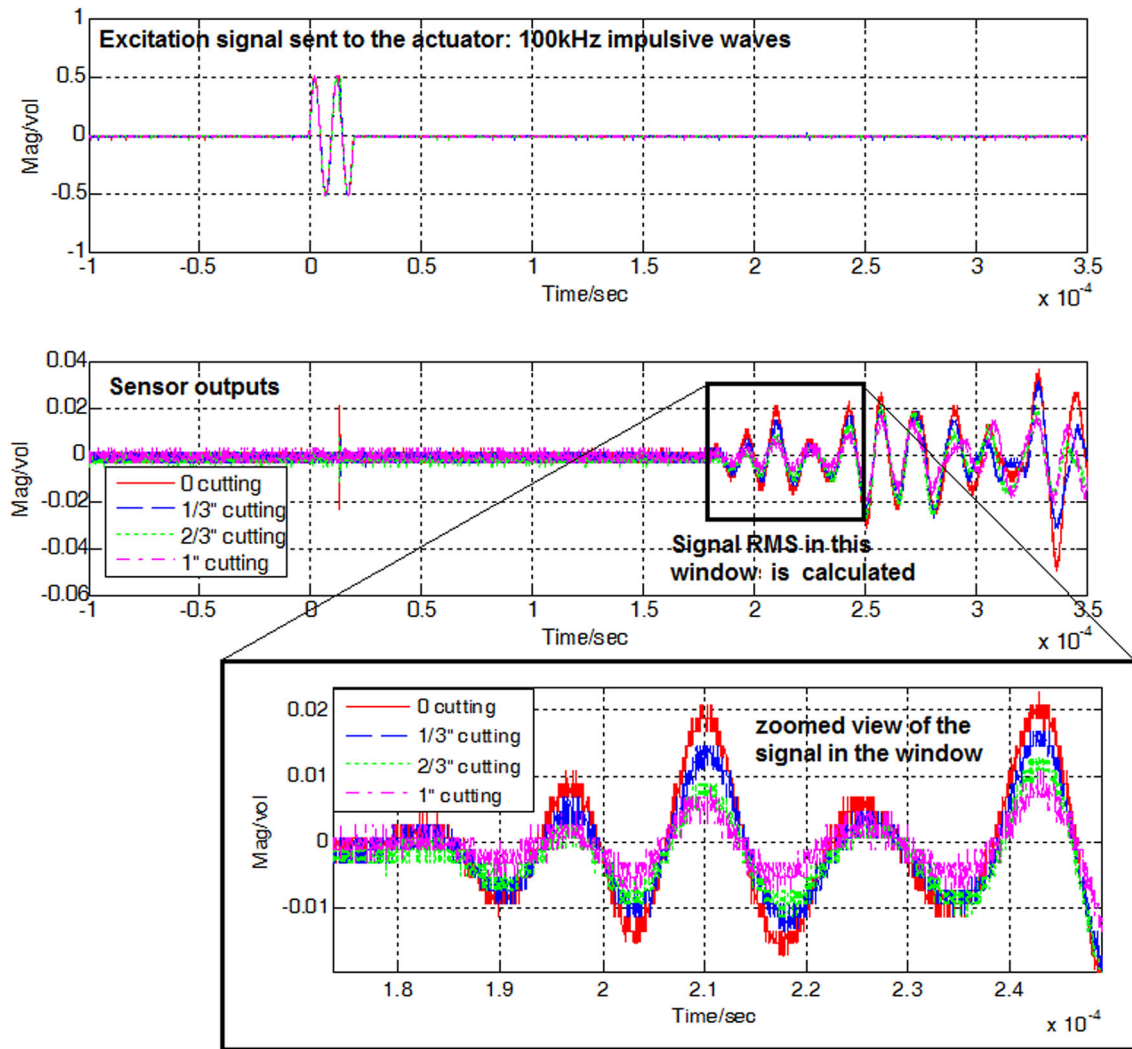


Fig. 5 Excitation signal and sensor response for 100 kHz excitation frequency

$$D \left(\frac{\partial^2}{\partial x^2} + \frac{\partial^2}{\partial y^2} \right) \langle E(x, y, t) \rangle - \frac{\partial}{\partial t} \langle E(x, y, t) \rangle - \sigma E(x, y, t) = p(x, y, t) \tag{2}$$

In this research, the Neumann boundary condition (zero flux across the boundaries) is enforced at the specimen boundaries [29]. The series solution of Eq. (2) for the source located at (x_0, y_0) is given by [22]:

$$E(x, y, t) = \left\{ 1 + \sum_{n=1}^{\infty} \sum_{m=1}^{\infty} 4 \cos\left(n\pi \frac{x_0}{l}\right) \cos\left(m\pi \frac{y_0}{p}\right) \times \cos\left(\frac{n\pi x}{l}\right) \cos\left(\frac{m\pi y}{p}\right) e^{-Dt((n\frac{\pi}{l})^2 + (m\frac{\pi}{p})^2)} + \sum_{n=1}^{\infty} 2 \cos\left(n\pi \frac{x_0}{l}\right) \cos\left(n\pi \frac{x}{l}\right) e^{-Dt(n\frac{\pi}{l})^2} + \sum_{m=1}^{\infty} 2 \cos\left(m\pi \frac{y_0}{p}\right) \cos\left(m\pi \frac{y}{p}\right) e^{-Dt(m\frac{\pi}{p})^2} \right\} \times E_0 e^{-\sigma t} \tag{3}$$

where l and p are lateral dimensions of the concrete structure (0.675 and 0.078 m respectively), x_0 and y_0 indicate the location of ultrasonic actuator (0.035 and 0.039 m, respectively), x and y indicate the location where the energy is measured (i.e. the sensor location) (0.635 and 0.039 m respectively), the dimensions are shown in Fig. 2.

By applying Eq. (3), the influence of variation in D (ultrasonic diffusivity coefficient) and σ (viscoelastic dissipation coefficient) on the detected energy (sensors responses) is evaluated and the results are shown in Figs. 6 and 7.

From Figs. 6 and 7, it is obvious that the diffusivity coefficient (D) has a more significant influence on the detected energy than dissipation (σ) which indicates that the diffusivity coefficient is a more sensitive parameter to the inhomogeneity in concrete structure and therefore feasible to be applied to detect cracks and evaluate the health status of concrete structures.

Fig. 6 Influence of diffusivity coefficient (D) on the sensor’s energy responses

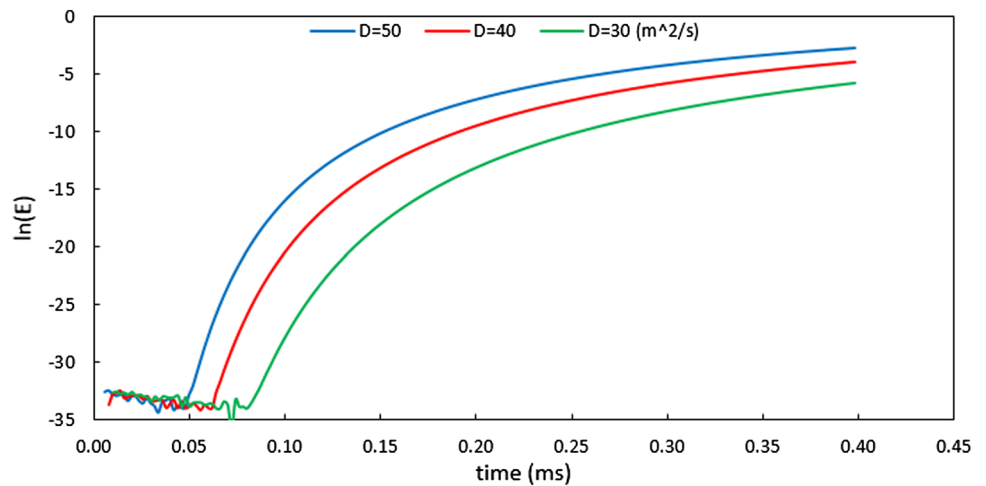
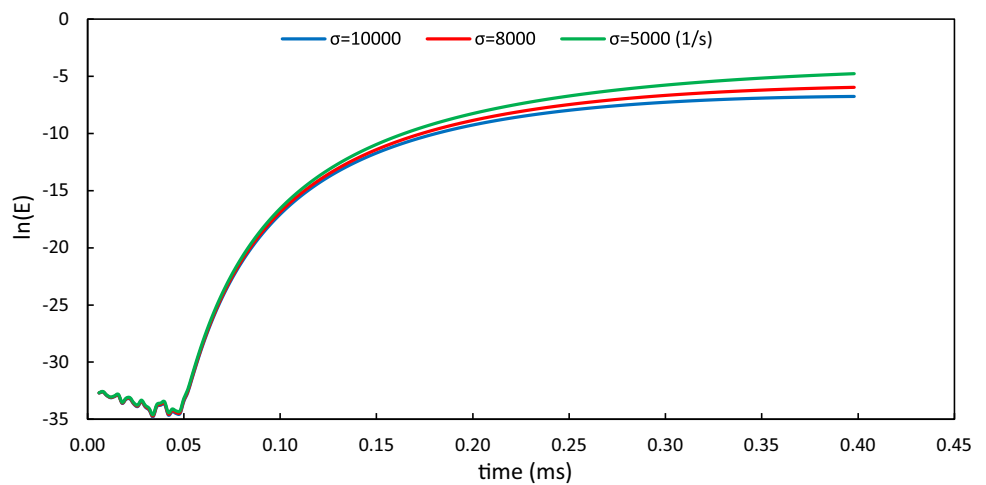


Fig. 7 Influence of dissipation coefficient (σ) on the sensor’s energy responses



4.3 Root mean square (RMS) calculation

To quantitatively describe the energy density of the signals, the RMS of the sensor responses is calculated with:

$$RMS = \sqrt{\frac{1}{T2 - T1} \sum_{T1}^{T2} [f(t) - \overline{f(t)}]^2} \tag{4}$$

where $T1$ and $T2$ are the start and end point of the dedicated window width. The RMS values of the signals in Figs. 4 and 5 are shown in Table 3.

Figure 8 shows the percentage of changes of the RMS and thus shows the variation of energy densities.

From the results above, it can be concluded that the cutting in the concrete will have significant influence on the sensor response. Considering the complexity of ultrasound propagation and experimental error, the RMS value of the detected signal decreases linearly with the cut depth, and the changes are significant, e.g., the RMS values are

Table 3 RMS values of different cut depth with different excitation frequencies

Excitation freq.	Cutting depth			
	0"	1/3"	2/3"	1"
50 kHz	0.0080	0.0062	0.0047	0.0036
100 kHz	0.0079	0.0059	0.0044	0.0030

reduced by more than 50 % under a 1" cut depth. While the 100 kHz excitation signal gave higher sensitivity as expected, both 50 kHz and 100 kHz excitation signals can detect cutting size of 1/3". It should be noted that the 1/3" cutting depth does not mean a cutting size of 1/3" as the cutting was all through the width of the concrete beam, so the cutting is about 2.5" in width and 1/3" in depth. The detectable resolution of the 50 kHz ultrasonic is about 0.68", thus can detect this size of cutting.

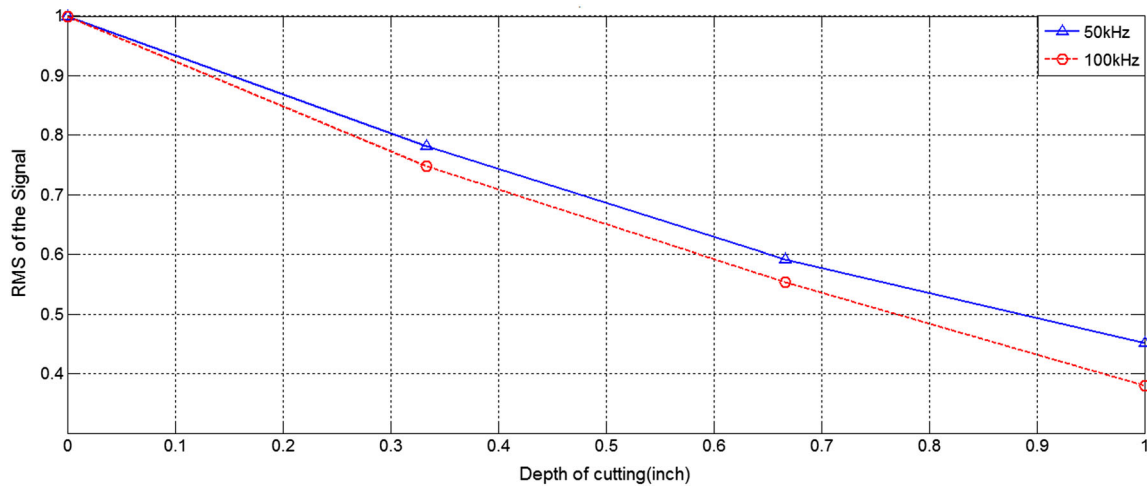


Fig. 8 RMS value change with different cutting depth for different excitation frequencies

Table 4 Properties of new concrete specimen

Made	W/C	Length	Width	Depth	Notch/depth	Age
Portland cement	0.38	82 cm	25 cm	2"	Max:0.5	>28 days

4.4 Detectable range analysis

To study the detectable range of the proposed system, a new concrete specimen was created and used. The properties of the new concrete specimen are shown in Table 4. The physical size and position of the components are shown in Fig. 9. From Fig. 9, it can be seen that Cut #1 is located at the side edge of the specimen, Cut #2 and 4 are located at the bottom side of the specimen, and both are a little bit away from the central line. The difference is the distance from “A” (actuator). Cut #3 is located on the path way between “A” (actuator) and “S1” (sensor #1). The depth of cutting is incrementally increased from 0" to 1", with an increment of 1/3". The other experimental components used in this experiment are the same as the previous one including the equipment and experiment procedures except the excitation frequencies were 20, 50, 100 k, and 200 kHz. It should be noted that cutting sequence is random and has no influence on the results. For each cutting, the RMS values are only influenced by the cutting depth and the previous cutting could be seen as a part of current structure.

Figure 10 shows the change of RMS values with Cut #1 with different cut depths for different excitation frequencies. Figures 11, 12, 13 show those of Cut #2, Cut #3, Cut #4, respectively. These results show that Cut #2 and Cut #3 have a consistently decreasing trend in RMS values which indicates that both Cut #2 and Cut #3 are detectable by this system. However, Cut #1 and Cut #4 did not give consistent output changing patterns. Considering both Cut #2,

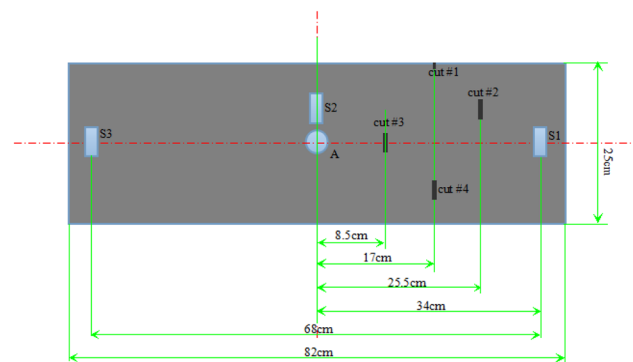


Fig. 9 Physical size and position of the experiment components from bottom view

Cut #3 and Cut #1, Cut #4 have the same cutting size (crack size) the reason that they have different RMS changing pattern is their locations which are a little far away from the central line between the actuator and sensor. Figure 14 shows the locations of the cuts and their angles off the central line. Cut #3 is on the way of the pathway, thus has the largest output changes with cutting. Cut #2 has a relative small angle with the pathway compared to Cut #1 and Cut #4 ($\theta_1 \approx 36^\circ$, $\theta_2 \approx 16.7^\circ$, $\theta_4 \approx 20^\circ$). In other words, it appears that the sensing system has a detectable angular range of about $\pm 15^\circ$, thus an array of 12 sensors would be needed to cover a circular area. From Figs. 11 and 12, it is obvious that 50 kHz excitation frequency will have a more linear RMS changing pattern which is desired for accurate measurement.

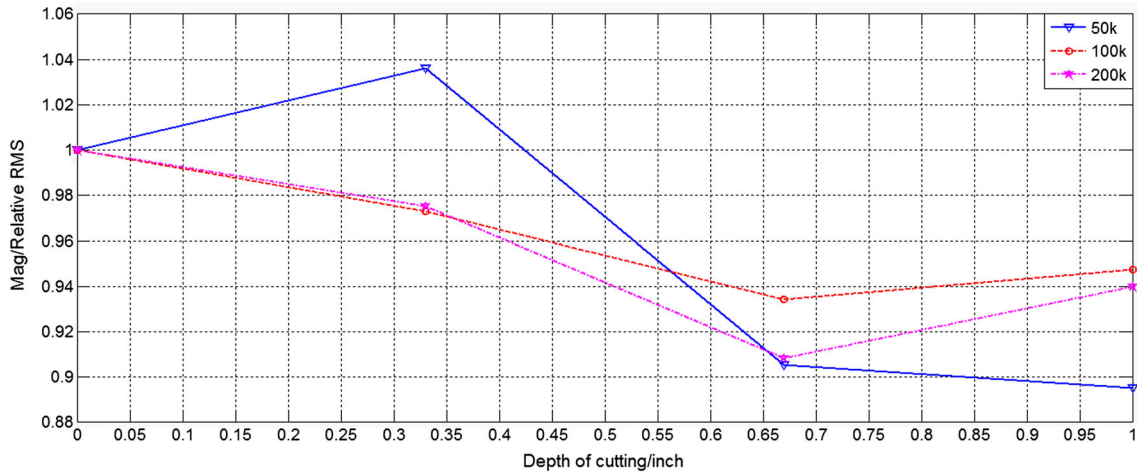


Fig. 10 RMS of sensor output for cut #1 (different lines are for different excitation frequencies)

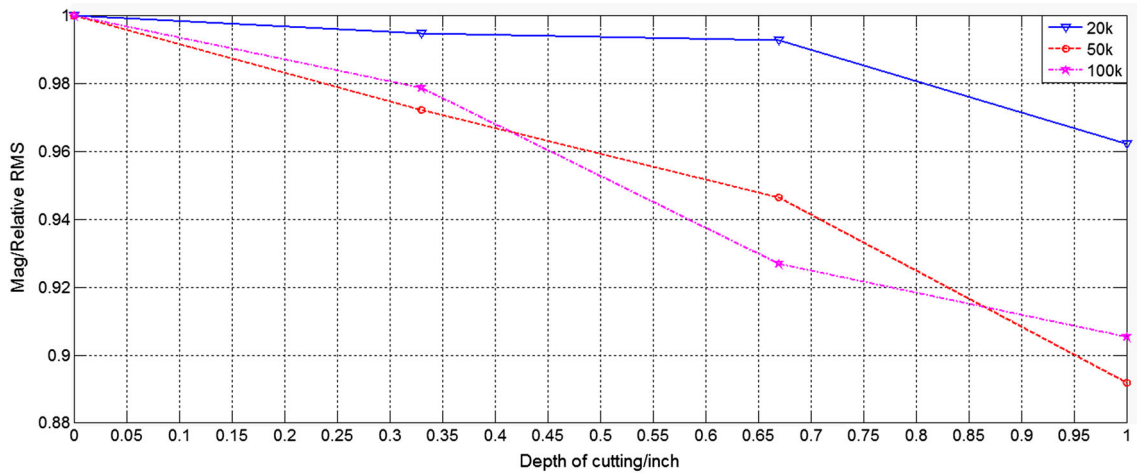


Fig. 11 RMS of sensor output for cut #2 (different lines are for different excitation frequencies)

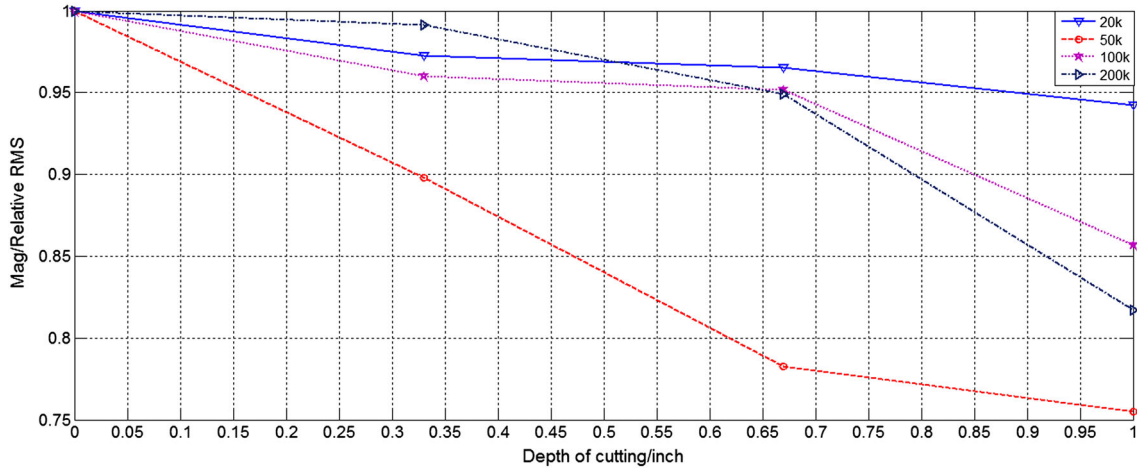


Fig. 12 RMS of sensor output for cut #3 (different lines are for different excitation frequencies)

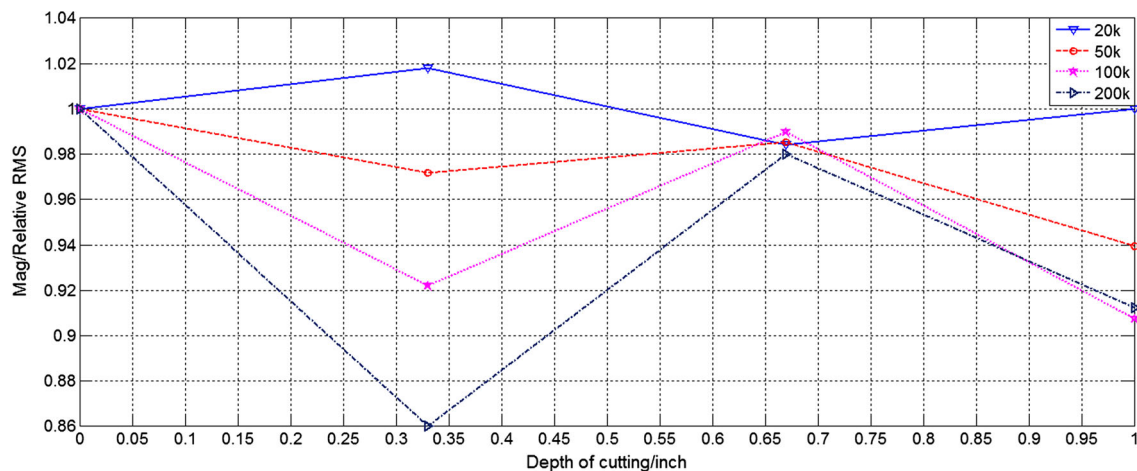
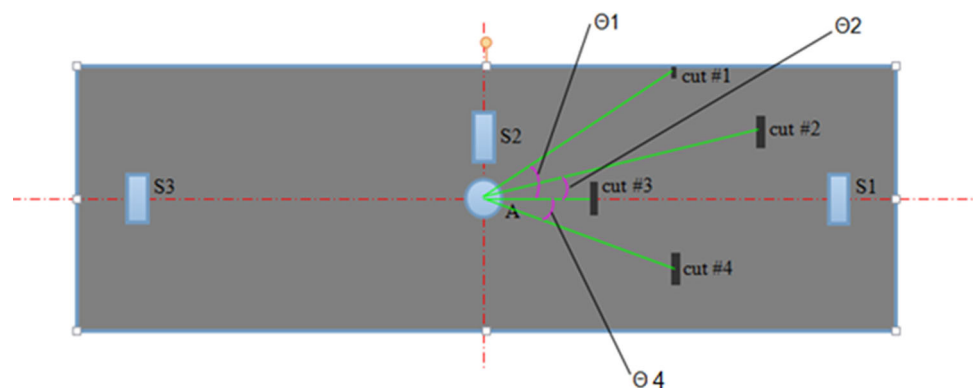


Fig. 13 RMS of sensor output for cut #4 (different lines are for different excitation frequencies)

Fig. 14 Locations of the cuts and their angles off the central line



5 Summary and conclusion

This paper presented experimental results of a piezoelectric active sensing system for concrete crack (cutting in the experiment) detection, which is based on the energy diffusivity method. Unlike impedance-based and Lamb wave-based approaches, the energy diffusivity-based approach pays more attention to the energy propagation property of ultrasound itself. From the analysis and experimental results, it can be concluded that it is feasible to apply diffusivity as a health monitoring index due to its high sensitivity to cutting depth. From RMS value calculation, it can be seen that energy diffusivity of the ultrasonic wave is inversely proportional to the cutting depth. In addition, it also displays a linearity between cutting depth and diffusivity which makes prediction of crack size more feasible. Even though some previous researchers have applied RMS as an index to indicate energy density during wave propagating through cuttings, they neglected the complexity of the sensor response and various noises in it and applied the whole signal to do the calculation. An effective window width of sensor response was proposed and found to give a

better performance using the RMS calculation. A subsequent experiment is carried out to study the detectable range using the proposed sensing system with this approach. Saw cuttings were arranged to be distributed at different distance from the actuator and different angles with the central line. A $\pm 15^\circ$ circular sector was proven to be the effective detectable range of the sensing system. With an array of sensors circularly placed around an actuator, a damage index can be calculated to assess the overall pavement health conditions of a large area of pavement. It should be noted that application of this sensing system in field requires further consideration. The moisture and temperature influence on the RMS index will be tested in the next step. Moreover, wireless signal interrogation techniques will be implemented with the system to achieve the goal of in situ monitoring of the health status of highway and airport pavement slabs.

Acknowledgments The authors would like to thank the US Federal Aviation Administration Airport Pavement R&D Section (Grant#: 2013G022) for funding support. The contents of the paper do not necessarily reflect the official views or policies of the FAA. The paper does not constitute a standard, specification, or regulation.

References

- Fujita Y, Mitani Y, Hamamoto Y (2006) A method for crack detection on a concrete structure. In: The 18th international conference on pattern recognition
- Fujita Y, Hamamoto Y (2011) A robust automatic crack detection method from noisy concrete surface. *Mach Vis Appl* 22:245–254
- Ito A, Aoki Y, Hashimoto S (2002) Accurate extraction and measurement of fine cracks from concrete block surface image. *Ind Electron Soc* 3:2202–2207
- Abdel-Qader I, Abudayyeh O, Kelly ME (2003) Analysis of edge-detection techniques for crack identification in bridges. *J Comput Civil Eng* 7(4):255–263
- Seung-Nam Yu, Jang J-H, Han C-S (2006) Auto inspection system using a mobile robot for detecting concrete cracks in a tunnel. *Auto Constr* 16(2007):255–261
- Yamaguchi T, Hashimoto S (2006) Automated crack detection for concrete surface image using percolation model and edge information. In: IEEE industrial electronics, IECON 2006, 32nd annual conference on, 3355–3360
- Sinha SK, Fieguth PW (2006) Automated detection of cracks in buried concrete pipe images. *Auto Constr* 15(2006):58–72
- Song G, Haihang G, Mo Y-L (2008) Smart aggregates: multi-functional sensor for concrete structures—a tutorial and a review. *Smart Mater Struct* 17(2008):1–17
- Gu H, Moslehy Y, Sanders D, Song G, Mo YL (2010) Multi-functional smart aggregate-based structural health monitoring of circular reinforced concrete columns subjected to seismic excitations. *Smart Mater Struct* 19:065026 (, p 7)
- Quinn W, Kelly G, Barrett J (2012) Development of an embedded wireless sensing system for the monitoring of concrete. *Struct Health Monit* 11:381–392
- Zhang Y (2006) In situ fatigue crack detection using piezoelectric paint sensor. *J Intell Mater Syst Struct* 2006(17):843
- Chong KP, Carino NJ, Washer G (2003) Health monitoring of civil infrastructures. *Smart Mater Struct* 12(2003):483–493
- Shin SW et al (2008) Piezoelectric sensor based nondestructive active monitoring of strength gain in concrete. *Smart Mater Struct* 17:1–8
- Wait JR, Park G, Farrar CR (2005) Integrated structural health assessment using piezoelectric active sensors. *Shock Vib* 12(6):389–405
- Park S, Ahmad S, Yun C-B, Roh Y (2006) Multiple crack detection of concrete structures using impedance-based structural health monitoring techniques. *Exp Mech* 46:609–618
- Zhu J, He L (2011) Piezoelectric actuator/sensor wave propagation based nondestructive active monitoring method of concrete structures. *J Wuhan Univ Technol Mater* 26(3):541–547
- Zhu J, Gao C, He L (2012) Piezoelectric-based crack detection techniques of concrete structures: experimental study. *J Wuhan Univ Technol Mater* 27(2):346–352
- Anugonda P, Wiehn JS, Turner JA (2001) Diffusion of ultrasound in concrete. *Ultrasonic J A* 39(6):429–435
- Deroo F, Kim J-Y, Qu J, Sabra K, Jacobs LJ (2010) Detection of damage in concrete using diffuse ultrasound. *J Acoust Soc Am* 127(6):3315–3318
- Anugonda P, Wiehn JS, Turner JA (2001) Diffusion of ultrasound in concrete. *Ultrasonics* 39(2001):429–435
- Turner J (1998) Diffusion of ultrasound in concrete. *J Acoust Soc Am* 104(3):1790
- Ramamoorthy SK, Kane Y, Turner JA (2004) Ultrasound diffusion for crack depth determination in concrete. *J Acoust Soc Am* 115(2):523–529
- Weaver RL (1990) Diffusivity of ultrasound in polycrystals. *J Mech Phys Solids* 38(1):55–86
- Weaver RL (1998) Ultrasonics in an aluminum foam. *Ultrasonics* 36(1–5):435–442
- Kee S-H, Zhu J (2013) Using piezoelectric sensors for ultrasonic pulse velocity measurements in concrete. *Smart Mater Struct* 22:115016 (, p 11)
- Demirboga R, Turkmen I, Karakoc MB (2004) Relationship between ultrasonic velocity and compressive strength for high-volume mineral-admixed concrete. *Cem Concr Res* 34(2004):2329–2336
- Ye G, Lura P, van Breugel K, Fraaij ALA (2004) Study on the development of the microstructure in cement-based materials by means of numerical simulation and ultrasonic pulse velocity measurement. *Cement Concr Compos* 26:491–497
- Schubert F, Koehler B (2004) Numerical time-domain simulation of diffusive ultrasound in concrete. *Ultrasonics* 42(1):781–786
- Casten RG, Holland CJ (1978) Instability results for reaction diffusion equations with Neumann boundary conditions. *J Differ Equ* 27(2):266–273